

Accepted Article

Title: Engineering Anti-CRISPR Proteins to Create Cas12a Protein Switches for Activatable Genome Editing and Viral Protease Detection

Authors: Wenyuan Kang, Fei Xiao, Xi Zhu, Xinyu Ling, Shiyi Xie, Ruimiao Li, Peihang Yu, Linxin Cao, Chunyang Lei, Ye Qiu, Tao Liu, and Zhou Nie

This manuscript has been accepted after peer review and appears as an Accepted Article online prior to editing, proofing, and formal publication of the final Version of Record (VoR). The VoR will be published online in Early View as soon as possible and may be different to this Accepted Article as a result of editing. Readers should obtain the VoR from the journal website shown below when it is published to ensure accuracy of information. The authors are responsible for the content of this Accepted Article.

To be cited as: *Angew. Chem. Int. Ed.* **2024**, e202400599

Link to VoR: <https://doi.org/10.1002/anie.202400599>

RESEARCH ARTICLE

Engineering Anti-CRISPR Proteins to Create Cas12a Protein Switches for Activatable Genome Editing and Viral Protease Detection

Wenyuan Kang,^[a,b] Fei Xiao,^[a] Xi Zhu,^[c] Xinyu Ling,^[d] Shiyi Xie,^[a] Ruimiao Li,^[a] Peihang Yu,^[a] Linxin Cao,^[a] Chunyang Lei,^{*[a]} Ye Qiu,^[c] Tao Liu^[d] and Zhou Nie^{*[a]}

- [a] Dr. W. Kang, F. Xiao, S. Xie, R. Li, P. Yu, L. Cao, Prof. C. Lei, Prof. Z. Nie
State Key Laboratory of Chemo/Biosensing and Chemometrics, College of Chemistry and Chemical Engineering, Hunan Provincial Key Laboratory of Biomacromolecular Chemical Biology,
Hunan University
Changsha 410082 (P. R. China)
E-mail: niezhou.hnu@gmail.com (Z. Nie); cylei@hnu.edu.cn (C. Lei)
- [b] Dr. W. Kang
Key Laboratory of Tropical Medicinal Resource Chemistry of Ministry of Education & Key Laboratory of Tropical Medicinal Plant Chemistry of Hainan Province, College of Chemistry and Chemical Engineering
Hainan Normal University
Haikou 571158 (P. R. China)
- [c] X. Zhu, Prof. Y. Qiu
Hunan Provincial Key Laboratory of Medical Virology, Institute of Pathogen Biology and Immunology, College of Biology
Hunan University
Changsha 410082 (P. R. China)
- [d] Dr. X. Ling, Prof. T. Liu
State Key Laboratory of Natural and Biomimetic Drugs, School of Pharmaceutical Sciences
Peking University
38 Xueyuan Road, Haidian District, Beijing 100191 (P. R. China)

Supporting information for this article is given via a link at the end of the document.

Abstract: Proteins capable of switching between distinct active states in response to biochemical cues are ideal for sensing and controlling biological processes. Activatable CRISPR-Cas systems are significant in precise genetic manipulation and sensitive molecular diagnostics, yet directly controlling Cas protein function remains challenging. Herein, we explore anti-CRISPR (Acr) proteins as modules to create synthetic Cas protein switches (CasPSs) based on computational chemistry-directed rational protein interface engineering. Guided by molecular fingerprint analysis, electrostatic potential mapping, and binding free energy calculations, we rationally engineer the molecular interaction interface between Cas12a and its cognate Acr proteins (AcrVA4 and AcrVA5) to generate a series of orthogonal protease-responsive CasPSs. These CasPSs enable the conversion of specific proteolytic events into activation of Cas12a function with high switching ratios (up to 34.3-fold). These advancements enable specific proteolysis-inducible genome editing in mammalian cells and sensitive detection of viral protease activities during virus infection. This work provides a promising strategy for developing CRISPR-Cas tools for controllable gene manipulation and regulation and clinical diagnostics.

Introduction

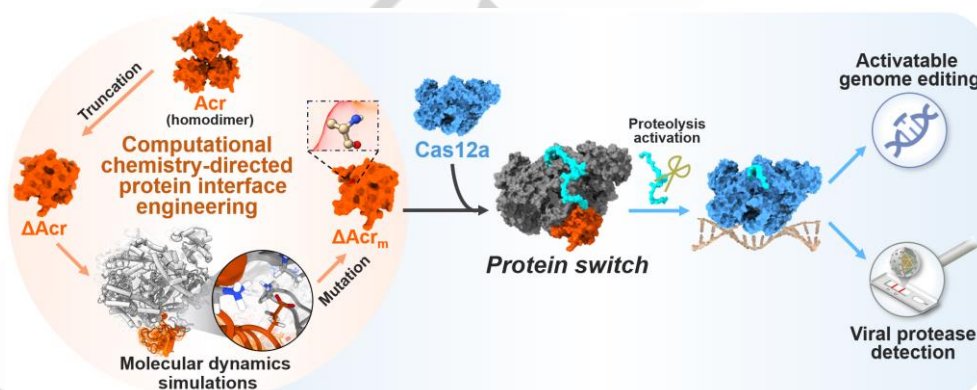
Synthetic protein switches with programmable response functions to specific molecular signals are indispensable for monitoring and controlling biological processes.^[1] Due to the programmability of RNA-guided target binding and processing by Cas proteins, CRISPR-Cas systems have become a versatile and revolutionary toolkit with widespread applications in genetic manipulation, bioimaging, and molecular diagnostics.^[2] However, the lack of adequate control over Cas protein function is a significant limitation, potentially resulting in off-target activity, highlighting the critical need for controllable CRISPR-Cas systems.^[3] Building on advancements in dynamic RNA technology and nucleic acid chemistry, researchers have developed conditional guide RNA (gRNA) whose activity depends on programmable triggers.^[4] This method regulates the CRISPR-Cas system by controlling gRNA activity rather than directly manipulating Cas protein function. For direct control of Cas protein function, Cas proteins are usually split into two parts and coupled with a stimulus-sensitive domain, requiring meticulous screening of split sites.^[5] While this approach offers a high level of controllability, the multidomain nature of routinely used Class 2 Cas proteins (e.g., Cas12a and Cas9) requires expertise in extensive protein engineering, rendering it a challenging endeavor with limited applicability and scalability. Therefore, there is an urgent need for a methodology that enables the practical and efficient creation of Cas protein switches.

RESEARCH ARTICLE

Bacteriophage-encoded anti-CRISPR (Acr) proteins, derived from the coevolutionary arms race between phages and bacterial immune systems, have emerged as a natural group of antagonistic agents that can inactivate CRISPR-Cas immune functions.^[6] Like Cas effectors, Acr proteins have a high degree of diversity, with nearly 100 families named after the corresponding CRISPR-Cas types they repress.^[7] Most Acr proteins inhibit CRISPR-Cas immunity by serving as physical barriers to prevent DNA binding or cleavage by corresponding Cas proteins. Meanwhile, specific Acr proteins can utilize enzymatic reactions to switch off Cas activities.^[8] Consequently, the Acr protein toolkit presents promising avenues for directly controlling Cas functions.^[9]

Nature has evolved robust mechanisms to execute zymogen-enzyme interconversion, primarily through proteolytic processes.^[10] The mechanisms are vital for enzymatic homeostasis and signal transduction, as exemplified by prothrombin activation in blood clotting and caspase activation during apoptosis.^[11] Typically, zymogens incorporate an intramolecular inhibitory domain to repress catalytic activity, with specific proteolytic cleavage triggering zymogen activation.^[12] By mimicking this naturally occurring mechanism, it is reasonable to assume that synthetic stimuli-responsive Cas protein switches could be constructed by intramolecularly coupling Cas protein with its cognate Acr protein. Remarkably, to our knowledge, such an attempt has not been previously reported. This research gap may be attributed to inherent defects of Acr proteins in constructing protein switches, including easy dimerization, high binding affinity, or enzymatically irreversible inhibition.^[9]

To address these challenges, we propose a computational chemistry-guided strategy to devise zymogen-mimicking synthetic Cas protein switches (CasPSs) using Acr proteins. As a proof of concept, we selected Cas12a and its corresponding Acr proteins as model systems, utilizing site-specific viral proteases as the triggering biochemical cues. Starting with AcrVA4, an Acr protein known for its strong dimerization tendency and high binding affinity toward Cas12a,^[13] we performed molecular fingerprint analysis and binding free energy calculations to gain insights into their molecular interaction interface (**Scheme 1**). With guidance from the computational chemistry calculations, we conducted truncation and alanine scanning mutation on AcrVA4, resulting in a panel of orthogonal CasPSs with tailored responses to specific viral proteases. We extended this approach to AcrVA5, an Acr protein that deactivates Cas12a via enzymatic acetylation.^[8] By employing electrostatic potential mapping, protein-protein docking, and binding free energy calculation, we effectively repurposed AcrVA5 as an inhibitory module to generate several AcrVA5-based CasPSs, showcasing the versatility and scalability of this strategy. These CasPSs displayed high switching ratios and good specificity, enabling proteolysis-inducible genome editing in mammalian cells upon activation by specific viral proteases. Furthermore, the CasPS-based assay displayed remarkable feasibility in detecting various viral proteases, such as analysis of 3C protease activities during the infection process of coxsackievirus B3. Therefore, this study established a computational chemistry-guided strategy for the rational construction of Cas protein switches, offering helpful tools for controlled genome modification and clinical diagnostics.



Scheme 1. Schematic of the rational construction of CasPS. Taking AcrVA4 as the model, based on comprehensive analysis and modulation of the molecular interaction interface between Cas12a and Acr protein, CasPS is developed by the intramolecular coupling of these two modules, allowing activatable genome editing and viral protease detection.

Results and Discussion

Construction of CasPS by intramolecular coupling of Cas12a with AcrVA4

To mimic the zymogen autoinhibition and activation mechanism, we first explored the possibility of constructing a CasPS by fusing the Cas protein with its corresponding Acr protein. In this endeavor, we sought to utilize tobacco etch virus (TEV) protease as a representative biomedical cue. A TEV protease cleavage site was incorporated into the peptide linker to devise CasPS_{TEV}, in

which Cas12a from *Lachnospiraceae bacterium* ND2006 (LbCas12a) and AcrVA4 are tethered into a fusion protein via the linker. However, a challenge emerged as AcrVA4 tended to form homodimers, leading to its binding with two molecules of the LbCas12a/gRNA complex.^[13a] This dimerization tendency could potentially impact the proteolysis activation process due to steric hindrance. To circumvent the potential side effects arising from the dimerization of wild-type AcrVA4 (**Fig. 1A**), we opted for a truncated version of AcrVA4 (Δ 1-133). This truncated variant (Δ AcrVA4) retained its inhibitory function while preventing dimer formation,^[13c] making it suitable for fusion with Cas12a (**Fig. 1A** and **1B**).

RESEARCH ARTICLE

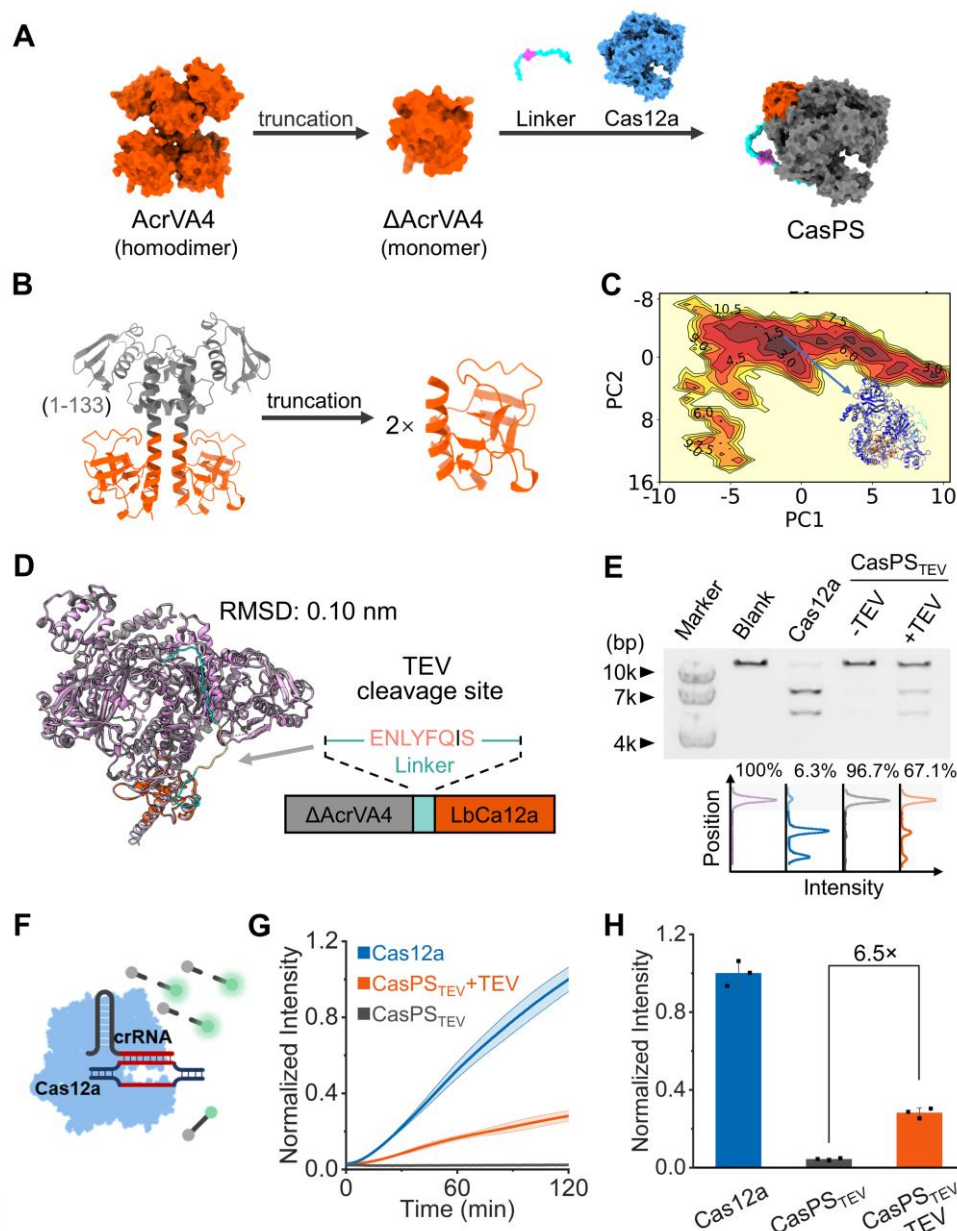


Figure 1. (A) Truncation of AcrVA4 to generate a monomer counterpart for constructing CasPS by intramolecularly coupling with Cas12a. (B) Illustration of the generation of monomeric Δ AcrVA4 by truncation (Δ 1-133). (C) FEL map depicting a low energy basin along with the representative structure of Δ AcrVA4-LbCas12a fusion protein. (D) The alignment of Δ AcrVA4-LbCas12a with the reported structure of AcrVA4/LbCas12a complex (PDB ID: 6OMV). (E) Analytical performance of CasPS_{TEV} by measuring Cas12a's *cis*-cleavage activity using gel electrophoresis. Cas12a, 40 nM; CasPS_{TEV}, 40 nM; gRNA 75 nM; linear plasmid, 60 ng; TEV protease, 0.1 U. The uncropped gel image was presented in the Supporting Information. (F) Scheme of the *trans*-cleavage of ssDNA reporters for signal reporting. (G-H) Evaluation of the *trans*-cleavage activity after the treatment of CasPS_{TEV} with TEV protease. CasPS_{TEV}, 50 nM; gRNA, 75 nM; dsDNA, 50 nM; TEV protease, 0.1 U; FQ reporter, 500 nM. Data represent means \pm SD ($n = 3$).

Utilizing the reported crystal structure of the Cas12a/AcrVA4 complex as a reference,^[13a] we analyzed their spatial orientation to guide the construction of CasPS_{TEV}. The distances between their termini were determined to be 5.98 nm (C_{Acr} to N_{Cas}) and 8.93 nm (C_{Cas} to N_{Acr}), respectively (Fig. S1). To minimize the peptide linker length, Δ AcrVA4 was fused to the N-terminal of Cas12a. Then, a rationally designed linker consisting of the cleavage site of TEV protease was used to construct CasPS_{TEV}, which was subjected to molecular dynamics simulation to assess the effect of fusion on protein-protein interactions (Fig. S2).^[14] The coordinates from the free energy landscape (FEL) maps with a minimum energy cluster were used to retrieve the low-energy

representative structure of CasPS_{TEV} (Fig. 1C).^[15] This structure was in alignment with the AcrVA4/Cas12a complex (Fig. 1D), theoretically demonstrating the feasibility of constructing CasPS by intramolecular coupling of Δ AcrVA4 and Cas12a.

Motivated by the computational assessment results, we next investigated the switching propriety of CasPS_{TEV}. We expressed and purified the designed CasPS_{TEV} and assessed the accessibility of its flexible linker to TEV protease by SDS-PAGE analysis (Fig. S3). Cas12a exhibits target-specific recognition and cleavage (*cis*-cleavage) activity as well as high collateral cleavage (*trans*-cleavage) activity over nearby single-stranded DNA (ssDNA).^[16] Thus, we quantified the specific proteolysis-

RESEARCH ARTICLE

responsiveness of CasPS_{TEV} based on the RNA-guided nuclease activities of Cas12a. As shown in **Fig. 1E**, the ratios of cleaved linear plasmid substrates in Cas12a and CasPS_{TEV} groups were 93.7% and 3.3%, respectively, suggesting a sharply prohibited *cis*-cleavage activity in CasPS_{TEV}. Meanwhile, the cleaved ratio was magnified to 32.9% upon the treatment with TEV protease, revealing a partial recovery in *cis*-cleavage activity. Using fluorophore/quencher-labeled ssDNA (FQ reporter) as the reporter, the *trans*-cleavage activity of Cas12a can be employed for the rapid evaluation of Cas12a function (**Fig. 1F**). The results shown in **Fig. 1G** and **1H** revealed that CasPS_{TEV} had a negligible *trans*-cleavage signal. On the contrary, the signal was magnified 6.5 times after TEV protease-mediated proteolysis. These data have demonstrated the responsiveness of Acr-based CasPS toward target protease-catalyzed proteolysis. However, only a partial restoration (approximately 30%) in both *cis*- and *trans*-cleavage signals were observed following target proteolysis. The moderate signal-to-background ratio observed in this experiment may be attributed to the intermolecular inhibition arising from the high affinity between the released AcrVA4 and Cas12a.^[13b] This suggests that further protein engineering efforts are required to enhance the switching efficiency.

Computational chemistry-directed protein interface engineering to improve switching ratios

To improve the switching ratio of CasPS, we aimed to rationally decrease the affinity between Δ AcrVA4 and Cas12a by fine-tuning their molecular interaction interface under the guidance of computational assessment (**Fig. 2A**). Using available crystal structures, we conducted molecular fingerprint analysis based on their binding interface (**Fig. 2B** and **S4**). Molecular fingerprint analysis revealed that the residues in Δ AcrVA4 that interacted most frequently ($\geq 90\%$) with Cas12a were E184, R187, E204, and R206 (**Fig. 2C** and **S5**). As hydrogen bond and electrostatic interactions were the major forces for these interactions, we performed alanine scanning mutations of the four residues to assess their contributions quantitatively.^[17] As shown in **Fig. 2D**, the relative binding free energy changes of E184A, R187A, E204A, and R206A were calculated to be 5.18 ± 1.88 , 0.87 ± 0.37 , 3.71 ± 0.92 , and 2.31 ± 1.07 kcal/mol, respectively. We first constructed the CasPS_{TEV} (E184A) variant that theoretically maximized the decrease in binding free energy among the single

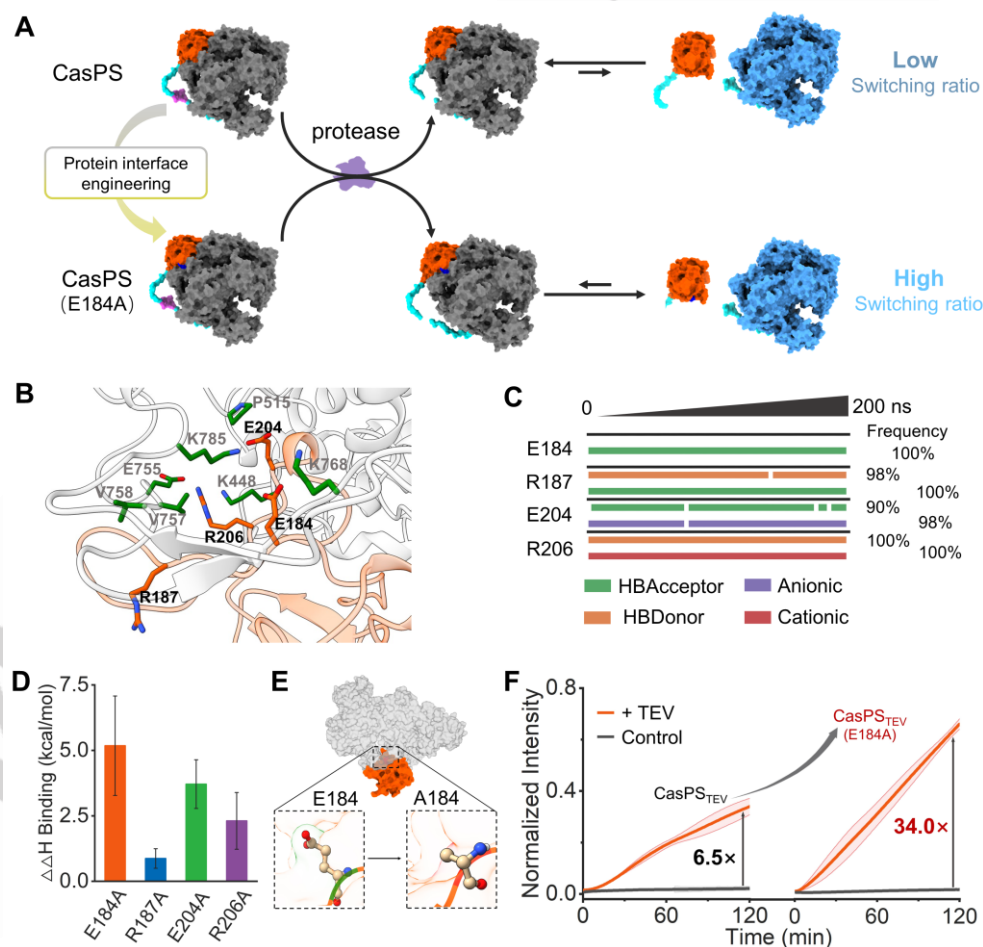


Figure 2. (A) Modulation of protein interaction interface to improve switching efficiency. (B) The interaction interface between Δ AcrVA4 (light orange) and LbCas12a (light grey) analyzed by UCSF ChimeraX. (C) The residues in Δ AcrVA4 interacting most frequently with LbCas12a determined by interaction fingerprint analysis. (D) Relative binding free energy changes of the four residues calculated by alanine scanning. (E) Scheme of the construction of CasPS_{TEV} (E184A). (F) Time-dependent *trans*-cleavage signals of CasPS_{TEV} and CasPS_{TEV} (E184A) upon the treatment with TEV protease. CasPS_{TEV} or CasPS_{TEV} (E184A), 50 nM; gRNA, 75 nM; dsDNA, 50 nM; TEV protease, 0.1 U; FQ reporter, 500 nM. Data represent means \pm SD (n = 3).

RESEARCH ARTICLE

mutations (Fig. 2E). Compared to the initial version, CasPS_{TEV} (E184A) exhibited a higher response signal (recovered 66.1% of Cas12a activity) with an even lower background, and thus the switching ratio improved from 6.5 to 34.0 (Fig. 2F). Moreover, other CasPS_{TEV} variants showed high switching ratios in the range of 25.5 - 34.3 folds (Fig. S6). Therefore, we have successfully improved the switching ratio of CasPS through computational chemistry-guided protein interface engineering, avoiding the need for tedious trial-and-error screening.

Furthermore, we investigated the impact of the linker on the performance of CasPS (Fig. 3A). As previously calculated in Fig. S1, the distance between AcrVA4 and Cas12a in CasPS is 5.98 nm, which is roughly equivalent to the length of a linear polypeptide consisting of 16 amino acid (aa) residues. To optimize the linker, we varied its length from 20 to 40 aa with a resolution of 10 aa and tested the switching ratios of CasPS variants based on the *trans*-cleavage signals. While all CasPS variants exhibited a strong response signal, we observed a significant increase in background signal when the linker length was reduced to 20 aa (Fig. S7). The AlphaFold2-constructed model showed that using the 20-aa linker prevented ΔAcrVA4 from effectively reaching the interaction site with Cas12a, leading to a weakened inhibitory effect (Fig. S8). The switching ratios of these CasPSs were

determined to be 3.2, 34.0, and 21.6, respectively (Fig. 3B). Consequently, we selected an optimized linker length of 30 aa for use in the following experiments.

To evaluate the versatility of this strategy, we aimed to create CasPS constructs capable of responding to different proteolytic cleavage cues. Viral proteases are a family of proteolytic enzymes encoded by many viruses and play a critical role in viral replication by cleaving specific viral polyproteins into their functional subunits. The CasPS could potentially detect viral infections by sensing the activity of viral proteases. To this end, we incorporated the substrate sequences of hepatitis C virus (HCV) NS3/4A protease and human rhinovirus (HRV) type 14 3C protease to generate CasPS_{NS3/4A} and CasPS_{3C} (Fig. S9), respectively. The molecular dynamics simulation results confirmed that the sequence replacements in the linker had negligible influence on protein-protein interaction interfaces (Fig. S10 and S11). Then, CasPS_{TEV}, CasPS_{NS3/4A}, and CasPS_{3C} were treated with these proteases, and the *trans*-cleavage signals were recorded. Each CasPS exhibited high switching ratios (27.8 - 34.3 folds, Fig. S12) and responded specifically to the corresponding viral protease with negligible crosstalk (Fig. 3C-E). Together, we have demonstrated that fine-tuning the linker sequence of CasPS enables versatile responsiveness to different sequence-specific viral proteases.

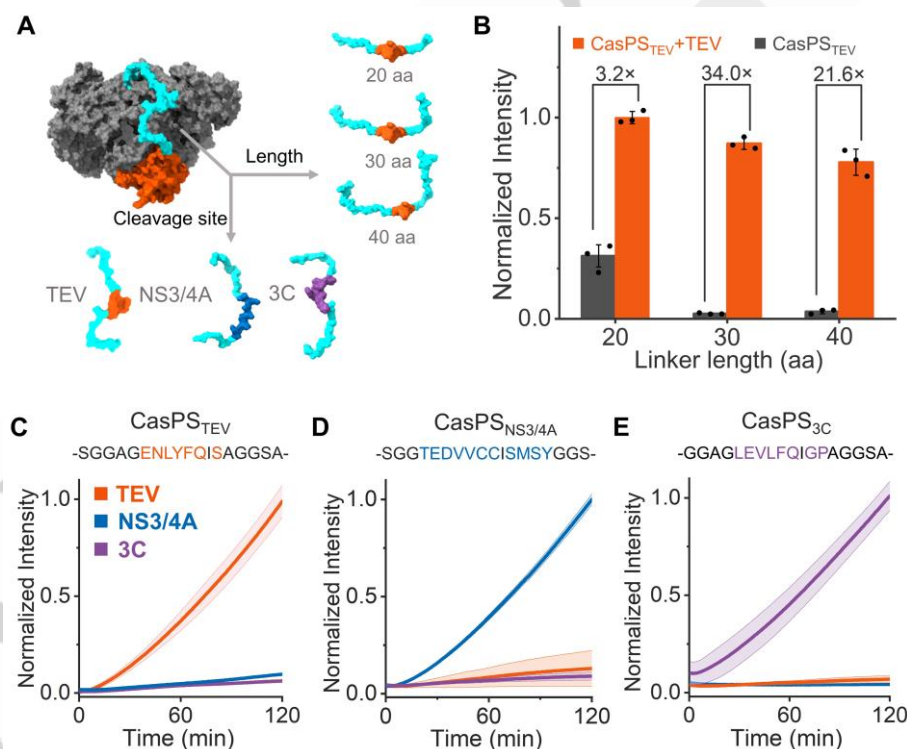


Figure 3. (A) Schematic illustration of the linker engineering with different lengths or cleavage sites. (B) The *trans*-cleavage signal intensities of CasPS_{TEV} with different linker lengths in response to TEV protease. CasPS_{TEV} with different linker lengths, 50 nM; gRNA, 75 nM; dsDNA, 50 nM; TEV, 0.1 U; FQ reporter, 500 nM. Evaluation of the response of (C) CasPS_{TEV}, (D) CasPS_{NS3/4A}, and (E) CasPS_{3C} in response to different proteases. CasPS, 50 nM; gRNA, 75 nM; dsDNA, 50 nM; FQ reporter, 500 nM; TEV protease, 0.1 U; HRV 3C protease, 0.05 U; HCV NS3/4A protease, 100 nM. Data represent means \pm SD (n = 3).

Construction of AcrVA5-based CasPSs

Inspired by the natural zymogen-enzyme interconversion mechanism, we have developed a modularized strategy for the design of CasPS and constructed a series of orthogonal CasPSs

based on AcrVA4. This design concept also suggests the possibility for employing alternative Acr proteins as inhibitory modules. Therefore, we next explore the applicability of this strategy to other Acr proteins, particularly those that are initially for Cas12a with acetyltransferase activity,^[8] as the model (Fig. 4A). AcrVA5 can catalyze the acetylation of a critical lysine

RESEARCH ARTICLE

residue in Cas12a, resulting in the loss of protospacer adjacent motif (PAM) recognition ability. To construct AcrVA5-based CasPSs, we need to accomplish the following two tasks: (1) determine the molecular interaction interface between AcrVA5 and Cas12a; (2) eliminate the irreversible inhibition of Cas12a caused by the acetyltransferase activity of AcrVA5.

We first analyzed the molecular interaction between AcrVA5 and Cas12a. Electrostatic potential mapping of AcrVA5 revealed a negatively charged environment surrounding the catalytic site, while the channel in Cas12a housing the lysine residue displayed a strong positive charge distribution (Fig. 4B and Fig. S13). This observation led us to propose the existence of an electrostatic interaction between AcrVA5 and Cas12a. Since there was no available crystal structure of the AcrVA5/Cas12a complex, we

employed molecular electrostatic potential (MESP) surface analysis and protein-protein docking to predict their interaction based on their reported structures (Fig. S14).^[18] Our findings indicated that the hydrophobic residues Y55 and L88 of AcrVA5 are inserted into the lumen of LbCas12a, potentially contributing to the acetyltransferase activity of AcrVA5 through nonpolar interactions (Fig. 4C). Moreover, the amino group of K595 (acetylation site) in LbCas12a forms hydrogen bonds with Y55, D80 and D82 in AcrVA5. Additionally, the flexible loop of AcrVA5 contains negatively charged amino acid residues (D80 and D82), which can engage in electrostatic interactions with the positively charged cavity of LbCas12a. These findings reveal that AcrVA5 could bind stably within the PAM binding cavity of LbCas12a in addition to its role as an acetyltransferase.

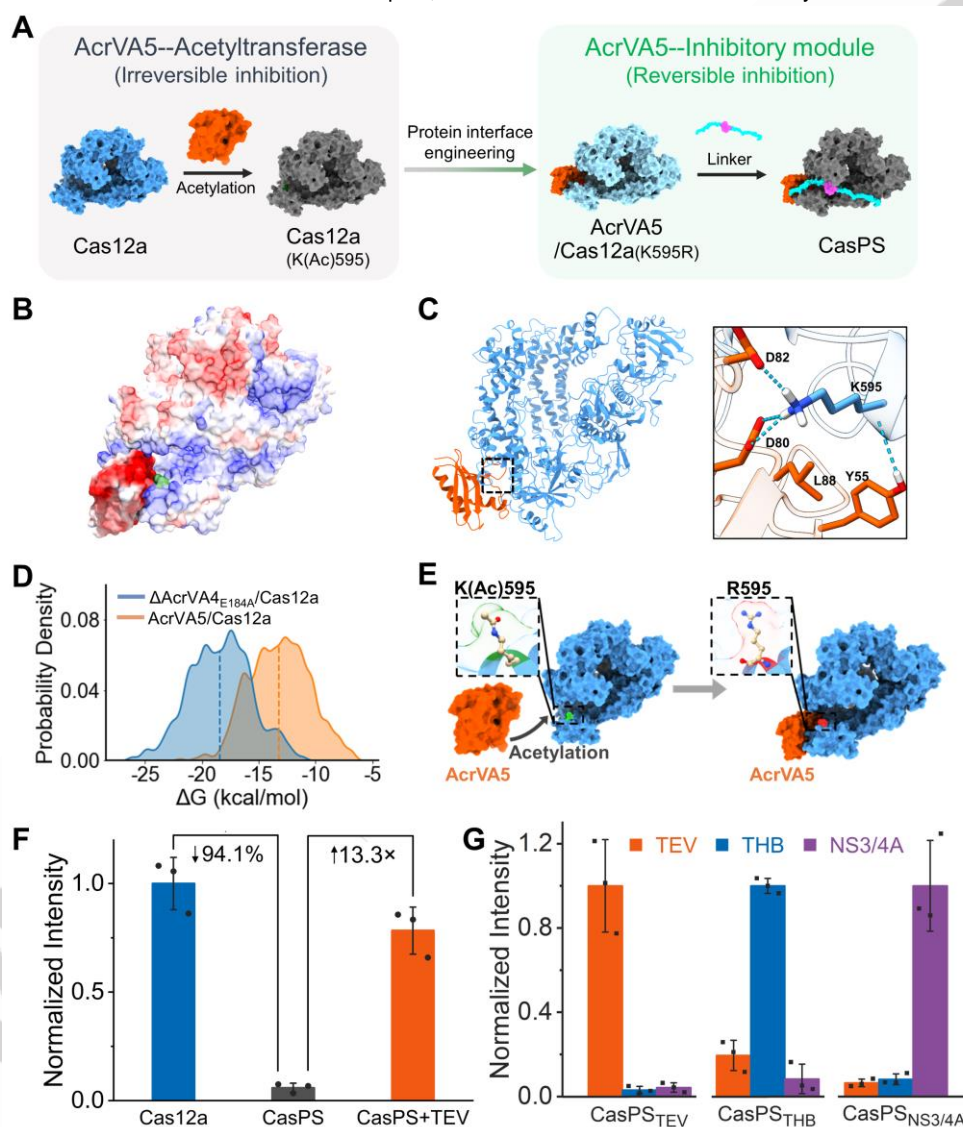


Figure 4. (A) Scheme of the construction of AcrVA5-based CasPS. (B) Electrostatic potential mapping of AcrVA5/LbCas12a complex. The complex was generated by protein-protein docking. (C) The interaction interface between AcrVA5 and LbCas12a analyzed by UCSF ChimeraX. (D) The calculated binding free energy of the AcrVA5/Cas12a complex and its comparison with that of the ΔAcrVA4_{E184A}/Cas12a complex. (E) Scheme of the construction of CasPS_{TEV} (K595R). (F) The *trans*-cleavage signal intensities of AcrVA5-based CasPS_{TEV} without and with the treatment of TEV protease. CasPS, 50 nM; gRNA, 75 nM; dsDNA, 50 nM; FQ reporter, 500 nM; TEV protease, 0.1 U. (G) The *trans*-cleavage signals of AcrVA5-based CasPSs in response to different proteases. CasPS, 50 nM; gRNA, 75 nM; dsDNA, 50 nM; FQ reporter, 500 nM; TEV protease, 0.1 U; THB, 10 nM; HCV NS3/4A protease, 100 nM. Data represent means ± SD (n = 3).

RESEARCH ARTICLE

Subsequently, we subjected the most representative docked conformation to molecular dynamics simulation to calculate the binding free energy between the two proteins.^[19] The computed binding free energy of the AcrVA5/Cas12a complex was -13.2 ± 2.7 kcal/mol, which is slightly weaker than that of AcrVA4 (E184A)/Cas12a complex (-18.4 ± 2.7 kcal/mol, **Fig. 4D**). This relatively weakened affinity between AcrVA5 and Cas12a might contribute to obtaining a high response signal when used to construct CasPSs. Together, these computational calculations suggest the potential of AcrVA5 as an inhibitory module in CasPS construction.

The acetyltransferase activity of AcrVA5 can result in the irreversible deactivation of Cas12a upon intramolecular coupling, making it impossible to restore Cas12a function through specific proteolytic cleavage. To overcome this obstacle, we modified their molecular interaction interface by substituting the key lysine residue (acetylation site) in LbCas12a with an arginine residue (K595R), a known substitution to have negligible effects on LbCas12a function.^[8] Molecular dynamics simulations revealed that the K595R substitution could maintain hydrogen bonding interactions with AcrVA5, as evidenced by the formation of hydrogen bonds with I21, G53, and Q59 in AcrVA5 (**Fig. S15**). Additionally, this substitution had an insignificant effect on binding free energy (**Fig. S16**). Guided by the conformation obtained by protein-protein docking, we intramolecularly coupled AcrVA5 to the C-terminal of Cas12a (K595R) to generate AcrVA5-based CasPSs (**Fig. 4E** and **Fig. S17**). Subsequently, CasPS for TEV protease was generated by incorporating the cleavage site into the linker. The liberation of Cas12a through specific proteolysis was confirmed by the appearance of the band corresponding to Cas12a upon treatment of CasPS_{TEV} with TEV protease, as observed in SDS-PAGE analysis (**Fig. S18**). The inhibition and subsequent recovery of Cas12a function were validated by monitoring the *trans*-cleavage signals of CasPS_{TEV} in the absence and presence of TEV protease (**Fig. 4F**). While this AcrVA5-based CasPS_{TEV} had a lower switching ratio of 13.3 compared to AcrVA4-based CasPSs, it exhibited a higher recovery rate of 78.3% in Cas12a activity. These observations could be linked with the relatively weaker affinity of AcrVA5 towards Cas12a, as calculated previously.

Similarly, CasPS variants for HCV NS3/4A protease and thrombin (THB) were generated by incorporating the corresponding proteolytic cleavage sequence into the linker. Then, the responses of these CasPSs to each protease were assessed to evaluate their specificities (**Fig. 4G**). All three AcrVA5-based CasPSs exhibited a strong response signal toward their cognate proteases with minimal crosstalk, suggesting the relatively high specificity of CasPSs for their intended targets. Collectively, these results highlight the general applicability of the proposed strategy for developing CasPSs using different Acr proteins.

CasPS for proteolysis-activated genome editing

Sequence-specific proteases have demonstrated versatility as foundational components for tools designed to monitor or regulate cellular functions. Protease-mediated biochemical circuits have been established for various applications, such as reporting cellular signaling and fine-tuning protein expression.^[20] Although protease-responsive Cas proteins are promising biochemical tools, their development is still in its infancy.^[5b] Encouraged by the effective performance of the specific proteolytic cleavage-activated CasPS *in vitro*, we explored its capabilities within cellular systems. We first assessed the potential of CasPS for activatable genome editing in mammalian cells using an enhanced green fluorescent protein (EGFP) disruption assay in HEK293-EGFP-TetOn cells (**Fig. 5A**).^[21] Specific plasmids were designed and constructed to separately express CasPS_{TEV} or TEV protease under a CMV promoter and crRNA under a U6 promoter (**Fig. S19**). In an initial test, HEK293-EGFP-TetOn cell lines were divided into four groups, each receiving a transient co-transfection with different vectors: (I) blank; (II) Cas12a and crRNA; (III) CasPS_{TEV}, crRNA, and catalytically inactive dTEV protease; and (IV) CasPS_{TEV}, crRNA, and TEV protease. After 24 h post-transfection, the expression of EGFP was induced by doxycycline for 24 h, and editing efficiency was quantified by flow cytometry. As shown in **Fig. 5B**, group III exhibited only a slight EGFP gene disruption, whereas the EGFP gene disruption efficiency in group IV was slightly lower than that of group II using a wild-type Cas12a. There is a significant difference in EGFP gene disruption levels between groups III and IV (**Fig. 5C**), demonstrating the preliminary implementation of target proteolysis-activated genome editing.

The potential of CasPS for genome editing was further evaluated by examining its ability to edit endogenous genes. The human HPRT1 (hHPRT1) locus in the HeLa cell line was selected as the target, and the standard T7 endonuclease 1 (T7E1) assay was used to quantify editing efficiencies (**Fig. S20**). Co-transfection of CasPS_{TEV} and TEV protease vectors resulted in an insertion-deletion (indel) efficiency of 30.0%, which was comparable to that of the positive control transfected with the Cas12a vector (**Fig. 5D**). In contrast, the group simultaneously transfected with CasPS_{TEV} and dTEV protease vectors showed a low background indel efficiency of 2.96%, and the switching ratio for the indel efficiency at hHPRT1 locus was determined to be 10.1. The remarkable difference in genome editing efficiency induced by TEV and dTEV proteases was consistent with the results of Sanger sequencing (**Fig. 5E**). Collectively, these results suggest that activatable genome editing triggered by specific proteolysis can be achieved with the use of CasPSs.

RESEARCH ARTICLE

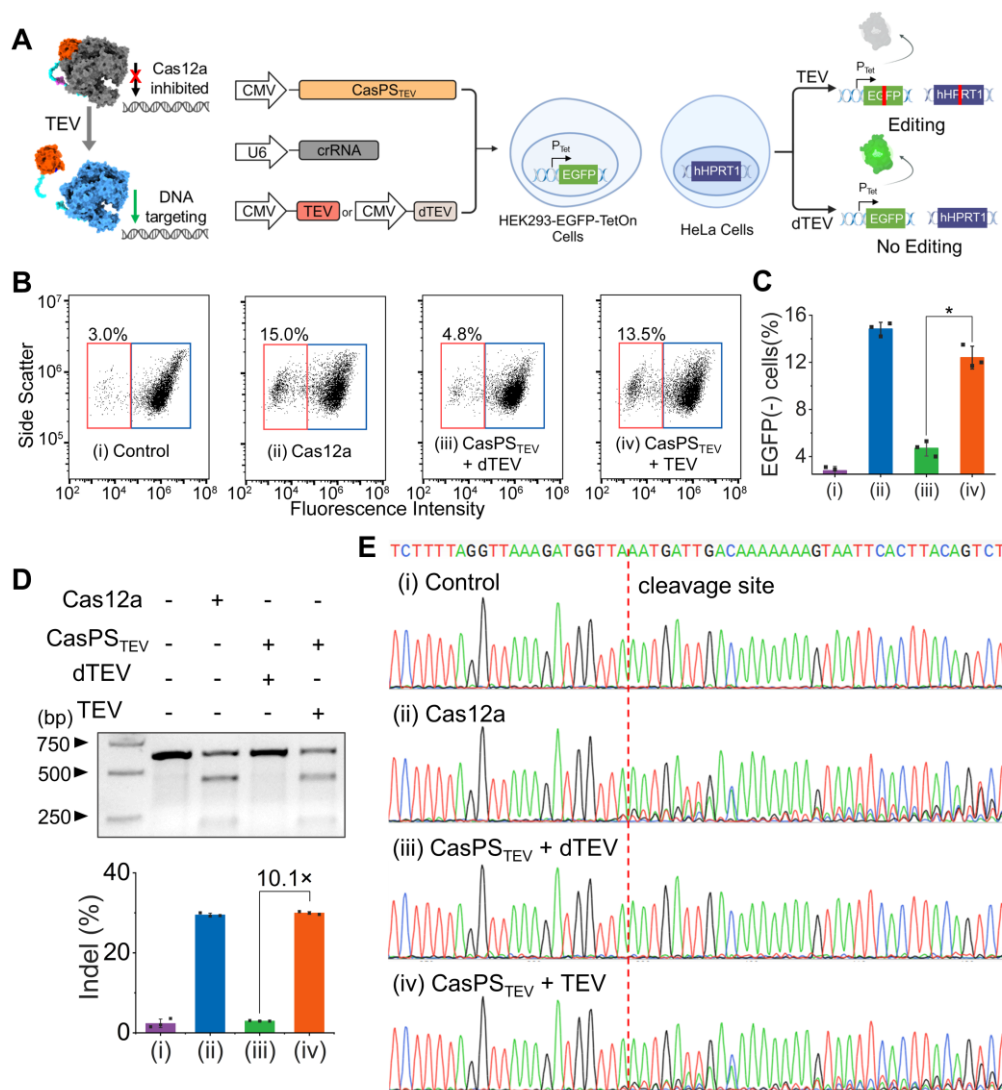


Figure 5. (A) Scheme of CasPS for proteolysis-activated genome editing. Produced by Figdraw. (B) Flow cytometry analysis of the HEK293-EGFP-TetOn cells after the treatment of a transient co-transfection with different vectors. (C) Background subtracted EGFP-negative proportions of HEK293-EGFP-TetOn cells upon different treatments. (D) Quantification of the mutation frequency of hHPRT1 locus in HeLa cells with different treatments by T7E1 assay. The uncropped gel image was shown in the Supporting Information. (E) Sanger sequencing traces from hHPRT1 locus in HeLa cells with different treatments. Data represent means \pm SD ($n = 3$). * $P < 0.05$, two-tailed Mann-Whitney test.

CasPS-based assay for viral protease detection

In addition to its widespread application in genome editing, the signal amplification capacity of Cas12a's *trans*-cleavage activity has also highlighted huge values for nucleic acid molecular diagnostics.^[22] However, the utility of the CRISPR-Cas12a system in protease biomarker detection has less explored.^[23] It is worth noting that the CasPSs can respond to cognate proteases directly, which might represent an alternative avenue to extend the application scope of CRISPR-Cas systems in diagnosing non-nucleic acid biomarkers.

The indispensable role of viral proteases in completing the viral infectious cycle prompted us to explore the utility of CasPS in profiling viral protease activity and viral infection.^[24] As shown in **Fig. 6A**, viral protease-mediated cleavage of CasPS restores the Cas12a function, triggering signal amplification through continuously cleaving ssDNA reporters with high turnovers. The

readout of signals can be monitored by fluorescence detection or naked-eye detection via lateral flow strip assay. As the major proteolytic enzymes of coronaviruses, picornaviruses, and enteroviruses, 3C cysteine proteases are involved in the proteolytic processing of polyproteins and interference with the cellular processes of host cells.^[25] Moreover, the 3C proteases are important drug targets in the development of antiviral therapies, and several drugs targeting the 3C protease have been developed and tested in clinical trials, such as rupintrivir for HRV and telaprevir and boceprevir for HCV.^[25b,c] Recently, the 3C protease of SARS-CoV-2, which is responsible for the COVID-19 pandemic, has also become a target for drug development.^[25d] Therefore, we tested the feasibility of CasPS in the sensitive detection of 3C protease activity and inhibitor screening. We determined the response of CasPS-based assay to 3C protease-mediated proteolytic cleavage, and the fluorescent signals showed a dose-dependent relationship with the concentration of

RESEARCH ARTICLE

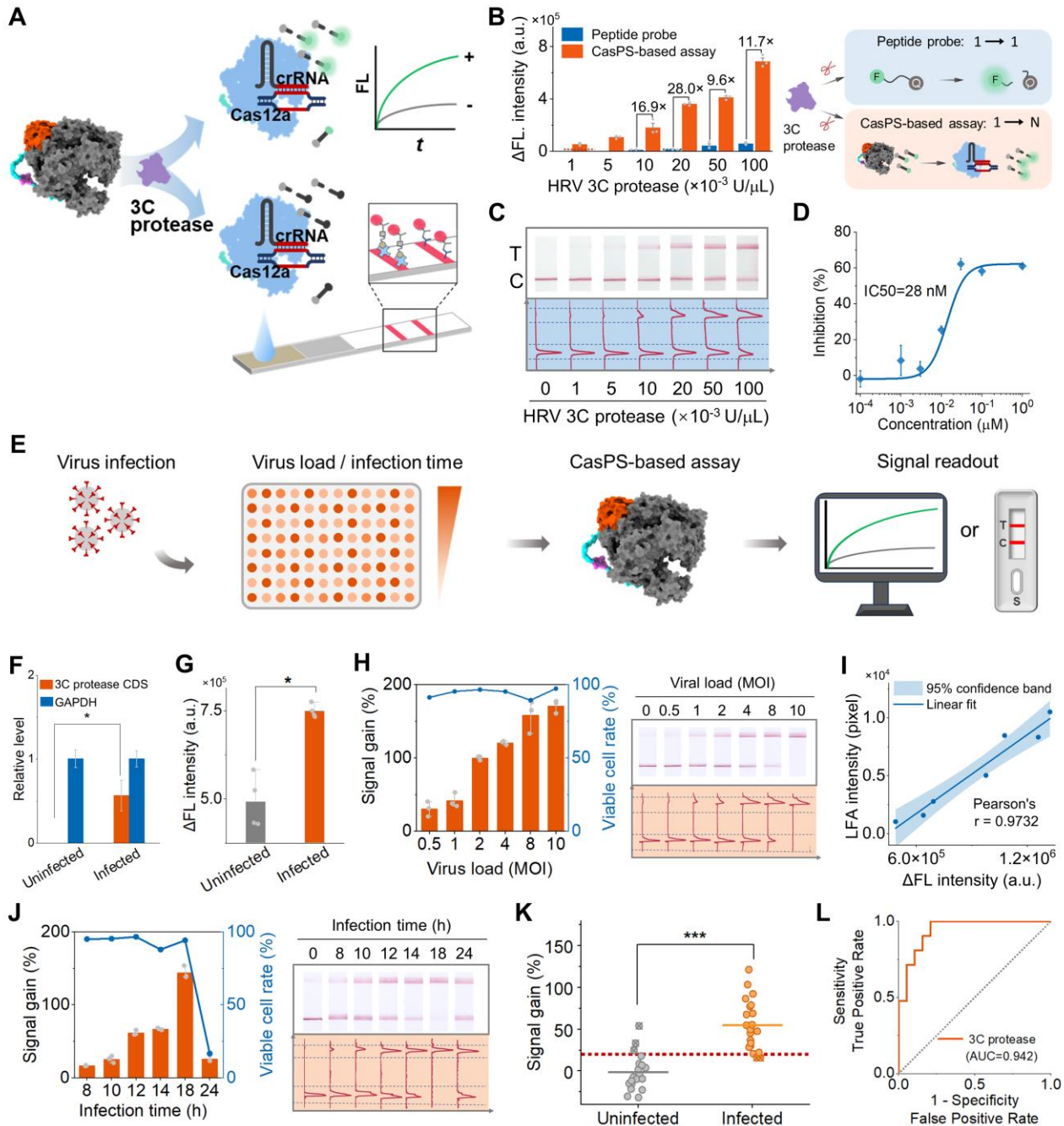


Figure 6. CasPS-based assay for viral protease detection. (A) Scheme of the CasPS-based assay for viral protease detection with fluorescent and lateral flow readouts. (B) Fluorescent response signals of CasPS- and peptide probe-based assays in response to varying concentrations of HRV 3C protease. The threshold lines represent the LOD calculated from blank controls' mean plus 3-fold standard deviations. (C) Lateral flow readouts of the CasPS-based assay responding to different concentrations of HRV 3C protease. (D) Inhibition curve of rupintrivir on HRV 3C protease determined by the CasPS-based assay. (E) Workflow of the CasPS-based assay for detecting 3C protease activity in biological samples. (F) The relative expression levels of 3C protease mRNA in infected and uninfected HEK293T cells quantified by qPCR. (G) Fluorescence response signals of the lysates from infected and uninfected HEK293T cells. (H) Fluorescent and lateral flow readouts of HEK293T cells infected by CVB3 with different MOI. (I) Correlation analysis between the fluorescent and lateral-flow readouts. (J) Fluorescent and lateral-flow readouts of infected HEK293T cells with different hpi. (K) The fluorescent responses of the 40 biological samples (19 uninfected samples and 21 CVB3-infected samples). (L) ROC analysis of the CasPS-based fluorescent readout detection accuracy in practical applications. Data represent means \pm SD (n = 3). * $P < 0.05$, *** $P < 0.001$, two-tailed Mann-Whitney test.

HRV 3C protease ranging from 1×10^{-3} to 100×10^{-3} U/ μ L (Fig. 6B). The limit of detection (LOD, 3σ rule) was calculated to be slightly less than 1×10^{-3} U/ μ L, over 20-fold lower than the conventional peptide probe-based assay (approximately 20×10^{-3}

U/ μ L). Moreover, the CasPS-based assay showed significantly increased response signals, ranging from 9.6 to 28.0 times higher than those observed in the peptide probe-based assay, due to the signal amplification stemming from Cas12a's *trans*-cleavage with

RESEARCH ARTICLE

a high turnover. The lateral flow readout showed increasing signals as the concentration of HRV 3C protease in the range of 10×10^{-3} - 100×10^{-3} U/ μ L. Using a commercially available HRV 3C protease inhibitor (rupintrivir) as the model, we demonstrated the utility of CasPS in sensing 3C protease inhibitors (Fig. 6D), indicating its potential usefulness in the development of anti-virus drugs.

Coxsackievirus B3 (CVB3) belongs to the *Picornaviridae* family and has been linked to human cardiac arrhythmias and viral myocarditis.^[26] Sequence and structure analysis revealed that coxsackievirus B3 (CVB3) 3C protease shares a high degree of homology with HRV 3C protease (Fig. S21 and S22), suggesting that the CasPS_{3C} could be employed as a valuable sensor to detect CVB3 3C protease activity. Here, we sought to explore the effectiveness of CasPS-based assay in assessing CVB3 3C protease activity in host cells after infection (Fig. 6E). Using HEK293T cells as the model, the efficacy of CVB3 infection was confirmed by quantitative real-time PCR (Fig. 6F and S23). The lysed cells were then subjected to the CasPS-based assay, and both the fluorescence and lateral flow readouts effectively distinguished infected from uninfected cells (Fig. 6G and S24).

As viral load and exposure time are important variables that affect the progress of infectious diseases, differentiating virus-infected cells with varying viral loads and infection times is essential for clinical diagnosis and treatment.^[27] To this end, we infected HEK293T cells with CVB3 at different multiplicities of infection (MOI) ranging from 0.5 to 10. The response signals showed a positive relationship with the amount of viral load in the fluorescence and lateral flow readouts (Fig. 6H). The two readouts exhibited a high degree of agreement, as indicated by Pearson's *r* of 0.9732 (Fig. 6I). Subsequently, the feasibility of the proposed assay in monitoring dynamic changes of 3C protease in cells after CVB3 infection was assessed by testing the infected cells at different hours post infection (hpi). As shown in Fig. 6J, the response signals continuously increased within 18 hpi, then sharply decreased at 24 hpi due to severe cell death at the late stage of CVB3 infection. To further validate the potential of CasPS in identifying CVB3 infection in practical scenarios, double-blind experiments were performed with 40 biological samples (19 uninfected samples and 21 CVB3-infected samples with different MOI ranging from 0.5 to 10). Positive and negative samples were identified based on a threshold value that represents the mean plus 3-fold standard deviations of the uninfected control. The overall statistical results (Fig. 6K, S25, and S26) showed 84.2% negative predictive agreement (specificity) and 90.5% positive predictive agreement (sensitivity). An area under the curve (AUC) value of 0.942 in the receiver operating characteristic (ROC) curve was calculated (Fig. 6L). Consequently, these data have demonstrated the feasibility of the CasPS-based assay in the detection of viral infections in complex biological samples.

Conclusion

In summary, this study presents a computational chemistry-guided approach to developing programmable Cas protein switches by engineering Acr proteins as modular components, drawing inspiration from zymogen autoinhibition and activation

mechanisms. Computational chemistry-guided rational protein interface engineering was employed to overcome inherent hurdles associated with constructing protein switches using Acr proteins. This effort resulted in the creation of a panel of orthogonal CasPSs with programmable response functions to specific proteolysis without the need for tedious trial-and-error screening. The approach presented in this study has achieved the facile and modularized generation of programmable and customizable Cas12a protein switches. The effectiveness of these CasPSs was demonstrated by their ability to perform activatable genome editing in mammalian cells and sensitive analysis of target protease activities during viral infections. The foundation of this strategy lies in the molecular interface interaction between Cas12a and its Acr proteins, potentially extending it to other class 2 Cas proteins in the future by fine-tuning the Cas-Acr protein pairs, such as Cas9-AcrIIA and Cas13-AcrVI.^[9] Furthermore, CasPS could be seamlessly integrated with stimuli-responsive vectors to achieve multiple stimuli-triggered activations of Cas functions^[3], enabling precise and intelligent control over CRISPR/Cas systems. Therefore, this work introduces a computational chemistry-directed approach to rationally construct Acr-based CasPSs, representing a promising strategy for developing controllable CRISPR-Cas tools for genetic manipulation, biochemical regulation, and clinical diagnostics.

Supporting Information

Details on materials and experimental procedures; the sequences of oligonucleotides and proteins; protein expression and purification; *in vitro cis/trans*-cleavage assays; molecular dynamics simulations; protein-protein docking.

Acknowledgements

This work was supported by the National Natural Science Foundation of China (22034002, 92253304, and 22374036), the National Key Research and Development Program of China (2020YFA0907500 and 2021YFA0910100), and the Hunan Provincial Natural Science Foundation of China (2022JJ20004). We thank Prof. Dali Li and Dr. Huiying Li at East China Normal University for helpful support and discussion about genome editing experiments.

Keywords: CRISPR-Cas • Anti-CRISPR Protein • Protein Switch • Viral Protease Detection • Protein Engineering

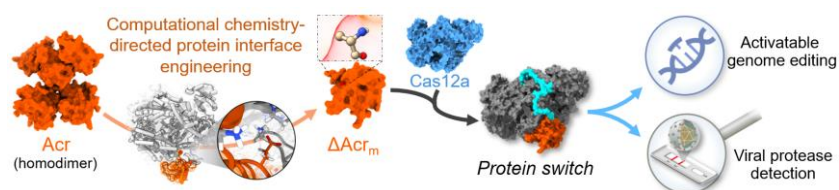
- [1] a) R. A. Langan, S. E. Boyken, A. H. Ng, J. A. Samson, G. Dods, A. M. Westbrook, T. H. Nguyen, M. J. Lajoie, Z. Chen, S. Berger, V. K. Mulligan, J. E. Dueber, W. R. P. Novak, H. El-Samad, D. Baker, *Nature* **2019**, *572*, 205–210; b) V. Stein, K. Alexandrov, *Trends Biotechnol.* **2015**, *33*, 101–110.
- [2] a) J. Y. Wang, P. Pausch, J. A. Doudna, *Nat. Rev. Microbiol.* **2022**, *20*, 641–656; b) A. Pickar-Oliver, C. A. Gersbach, *Nat. Rev. Mol. Cell Biol.* **2019**, *20*, 490–507; c) S. Chen, B. Gong, C. Zhu, C. Lei, Z. Nie, *TrAC Trends Anal. Chem.* **2023**, *159*, 116931; d) Y. Tang, L. Gao, W. Feng, C.

RESEARCH ARTICLE

- Guo, Q. Yang, F. Li, X. C. Le, *Chem. Soc. Rev.* **2021**, *50*, 11844–11869; e) K. Shi, S. Xie, R. Tian, S. Wang, Q. Lu, D. Gao, C. Lei, H. Zhu, Z. Nie, *Sci. Adv.* **2021**, *7*, eabc7802.
- [3] a) J. A. Doudna, *Nature* **2020**, *578*, 229–236; b) W. Cai, T. Luo, L. Mao, M. Wang, *Angew. Chem. Int. Ed.* **2021**, *60*, 8596–8606.
- [4] a) X.-W. Wang, L.-F. Hu, J. Hao, L.-Q. Liao, Y.-T. Chiu, M. Shi, Y. Wang, *Nat. Cell Biol.* **2019**, *21*, 522–530; b) W. Cai, J. Liu, X. Chen, L. Mao, M. Wang, *J. Am. Chem. Soc.* **2022**, *144*, 22272–22280; c) M. H. Hanewich-Hollatz, Z. Chen, L. M. Hochrein, J. Huang, N. A. Pierce, *ACS Cent. Sci.* **2019**, *5*, 1241–1249; d) L. Oesinghaus, F. C. Simmel, *Nat. Commun.* **2019**, *10*, 2092; e) Y. Sun, W. Chen, J. Liu, J. Li, Y. Zhang, W. Cai, L. Liu, X. Tang, J. Hou, M. Wang, L. Cheng, *Angew. Chem. Int. Ed.* **2023**, *62*, e202212413; f) S.-R. Wang, L.-Y. Wu, H.-Y. Huang, W. Xiong, J. Liu, L. Wei, P. Yin, T. Tian, X. Zhou, *Nat. Commun.* **2020**, *11*, 91.
- [5] a) Y. Xu, N. Tian, H. Shi, C. Zhou, Y. Wang, F.-S. Liang, *J. Am. Chem. Soc.* **2023**, *145*, 5561–5569; b) B. L. Oakes, C. Fellmann, H. Rishi, K. L. Taylor, S. M. Ren, D. C. Nadler, R. Yokoo, A. P. Arkin, J. A. Doudna, D. F. Savage, *Cell* **2019**, *176*, 254–267; c) Y. Nihongaki, T. Otabe, Y. Ueda, M. Sato, *Nat. Chem. Biol.* **2019**, *15*, 882–888.
- [6] N. D. Marino, J. Y. Zhang, A. L. Borges, A. A. Sousa, L. M. Leon, B. J. Rauch, R. T. Walton, J. D. Berry, J. K. Joung, B. P. Kleinstiver, J. Bondy-Denomy, *Science* **2018**, *362*, 240–242.
- [7] a) A. Pawluk, A. R. Davidson, K. L. Maxwell, *Nat. Rev. Microbiol.* **2018**, *16*, 12–17; b) N. D. Marino, R. Pinilla-Redondo, B. Csörgő, J. Bondy-Denomy, *Nat. Methods* **2020**, *17*, 471–479; c) H. Shivram, B. F. Cress, G. J. Knott, J. A. Doudna, *Nat. Chem. Biol.* **2021**, *17*, 10–19.
- [8] L. Dong, X. Guan, N. Li, F. Zhang, Y. Zhu, K. Ren, L. Yu, F. Zhou, Z. Han, N. Gao, Z. Huang, *Nat. Struct. Mol. Biol.* **2019**, *26*, 308–314.
- [9] N. Jia, D. J. Patel, *Nat. Rev. Mol. Cell Biol.* **2021**, *22*, 563–579.
- [10] M. C. Montasell, P. Monge, S. Carmali, L. M. Dias Loiola, D. G. Andersen, K. B. Løvschall, A. B. Søgaard, M. M. Kristensen, J. M. Pütz, A. N. Zelikin, *Nat. Commun.* **2022**, *13*, 4861.
- [11] a) M. F. Whelihan, V. Zachary, T. Orfeo, K. G. Mann, *Blood* **2012**, *120*, 3837–3845; b) N. Van Opendenbosch, M. Lamkanfi, *Immunity* **2019**, *50*, 1352–1364.
- [12] J. A. Gramespacher, A. J. Stevens, D. P. Nguyen, J. W. Chin, T. W. Muir, *J. Am. Chem. Soc.* **2017**, *139*, 8074–8077.
- [13] a) H. Zhang, Z. Li, C. M. Dackowski, C. Gabel, A. D. Mesecar, L. Chang, *Cell Host & Microbe* **2019**, *25*, 815–826; b) R. Peng, Z. Li, Y. Xu, S. He, Q. Peng, L. Wu, Y. Wu, J. Qi, P. Wang, Y. Shi, G. F. Gao, *Proc. Natl. Acad. Sci. U.S.A.* **2019**, *116*, 18928–18936; c) G. J. Knott, B. F. Cress, J.-J. Liu, B. W. Thornton, R. J. Lew, B. Al-Shayeb, D. J. Rosenberg, M. Hammel, B. A. Adler, M. J. Lobba, M. Xu, A. P. Arkin, C. Fellmann, J. A. Doudna, *eLife* **2019**, *8*, e49110.
- [14] S. Páll, A. Zhmurov, P. Bauer, M. Abraham, M. Lundborg, A. Gray, B. Hess, E. Lindahl, *J. Chem. Phys.* **2020**, *153*, 134110.
- [15] G. Mattedi, S. Acosta-Gutiérrez, T. Clark, F. L. Gervasio, *Proc. Natl. Acad. Sci. U.S.A.* **2020**, *117*, 15414–15422.
- [16] J. S. Chen, E. Ma, L. B. Harrington, M. Da Costa, X. Tian, J. M. Palefsky, J. A. Doudna, *Science* **2018**, *360*, 436–439.
- [17] M. S. Valdés-Tresanco, M. E. Valdés-Tresanco, P. A. Valiente, E. Moreno, *J. Chem. Theory Comput.* **2021**, *17*, 6281–6291.
- [18] a) S. Unni, Y. Huang, R. M. Hanson, M. Tobias, S. Krishnan, W. W. Li, J. E. Nielsen, N. A. Baker, *J. Comput. Chem.* **2011**, *32*, 1488–1491; b) C. Dominguez, R. Boelens, A. M. J. J. Bonvin, *J. Am. Chem. Soc.* **2003**, *125*, 1731–1737.
- [19] B. R. Miller, T. D. McGee, J. M. Swails, N. Homeyer, H. Gohlke, A. E. Roitberg, *J. Chem. Theory Comput.* **2012**, *8*, 3314–3321.
- [20] a) H. K. Chung, M. Z. Lin, *Nat. Methods* **2020**, *17*, 885–896; b) W. Cao, Z. Z. Geng, N. Wang, Q. Pan, S. Guo, S. Xu, J. Zhou, W. R. Liu, *Angew. Chem. Int. Ed.* **2022**, *61*, e202109550.
- [21] X. Ling, L. Chang, H. Chen, X. Gao, J. Yin, Y. Zuo, Y. Huang, B. Zhang, J. Hu, T. Liu, *Mol. Cell* **2021**, *81*, 4747–4756.
- [22] a) M. M. Kaminski, O. O. Abudayyeh, J. S. Gootenberg, F. Zhang, J. J. Collins, *Nat. Biomed. Eng.* **2021**, *5*, 643–656; b) S. Chen, R. Wang, S. Peng, S. Xie, C. Lei, Y. Huang, Z. Nie, *Chem. Sci.* **2022**, *13*, 2011–2020; c) M. Hu, C. Yuan, T. Tian, X. Wang, J. Sun, E. Xiong, X. Zhou, *J. Am. Chem. Soc.* **2020**, *142*, 7506–7513.
- [23] M. Yang, K. Shi, F. Liu, W. Kang, C. Lei, Z. Nie, *Sci. China Chem.* **2021**, *64*, 330–336.
- [24] L. Tong, *Chem. Rev.* **2002**, *102*, 4609–4626.
- [25] a) B. V. Tsu, E. J. Fay, K. T. Nguyen, M. R. Corley, B. Hosuru, V. A. Dominguez, M. D. Daugherty, *Front. Immunol.* **2021**, *12*, 769543; b) S. Yuan, K. Fan, Z. Chen, Y. Sun, H. Hou, L. Zhu, *Viral. Sin.* **2020**, *35*, 445–454; c) A. A. Butt, F. Kanwal, *Clin. Infect. Dis.* **2012**, *54*, 96–104. d) T. Miura, T. R. Malla, C. D. Owen, A. Tumber, L. Brewitz, M. A. McDonough, E. Salah, N. Terasaka, T. Katoh, P. Lukacik, C. Strain-Damerell, H. Mikolajek, M. A. Walsh, A. Kawamura, C. J. Schofield, H. Suga, *Nat. Chem.* **2023**, *15*, 998–1005.
- [26] F. S. Garmaroudi, D. Marchant, R. Hendry, H. Luo, D. Yang, X. Ye, J. Shi, B. M. McManus, *Future Microbiol.* **2015**, *10*, 629–653.
- [27] O. Puhach, B. Meyer, I. Eckerle, *Nat. Rev. Microbiol.* **2023**, *21*, 147–161.

RESEARCH ARTICLE

Entry for the Table of Contents



A panel of orthogonal protease-responsive Cas12a protein switches are presented by leveraging Anti-CRISPR proteins as modular components under the rational guidance of computational chemistry-directed protein interface engineering. The protein switches facilitate the conversion of specific proteolytic events into activation of Cas12a function high switching ratios, allowing activatable genome editing and sensitive viral protease detection.